

Low energy excitations in A-site ordered SmBaMn₂O₆

Mirian Garcia Fernandez^{1*}, Abhishek Nag^{1,2}, Stefano Agrestini¹, Sahil Tippireddy¹, Dirk Backes¹, Urs Staub³, Taka-hisa Arima⁴ and Kejin Zhou¹

¹*Diamond Light Source, Harwell Science and Innovation Campus, OX110DE, Didcot*

²*Department of Physics, Indian Institute of Technology Roorkee, Uttarakhand 247667, India*

³*Center for Photon Science, Forschungsstrasse 111,*

Paul Scherrer Institute, 5232 Villigen-PSI, Switzerland and

⁴*Department of Advanced Materials Science, University of Tokyo, Kashiwa 277-8561, Japan*

The electron in a solid can be considered a bound state of the three independent, fundamental degrees of freedom creating quasi-particles: spinons, carrying the electron spin; plasmons carrying the collective charge mode and orbitons carrying its orbital degree of freedom. These fundamental degrees of freedom could form ordering states in which dynamics or collective motions could occur and manifest as low-energy excitations. The exotic properties that appear in the materials exhibiting these electronic orderings are associated with these low-energy excitations. Although the orbital order (OO) and its coupling to the spin system creates very interesting phenomena, the microscopic origin of OO has been much less explored than other electronic properties as it is very difficult to directly access experimental information from OO. Due to the recent improvement in energy resolution and flux, soft x-ray resonant inelastic scattering (RIXS) allows for a re-examination of orbital excitations in manganites. Here, we present a study of low energy excitations in half doped A-site ordered SmBaMn₂O₆ through a combination of RIXS and soft x-ray resonant elastic scattering (REXS) measurements. The obtained experimental data confirm the OO at $\mathbf{q} = (0.25, 0.25, 0)$ and find various low energy excitations below 200 meV. While several excitations can be assigned to be of magnetic and phononic origin, a group of excitations between 80 and 200 meV show a temperature dependence distinctively following that of the OO making them possible candidates for orbital excitations.

I. INTRODUCTION

Quasiparticles characterize low energy excitations in strongly correlated electron systems. This concept is used to describe the collective behavior by treating it as a single particle which is important to simplify the many body problem. While fermionic quasiparticles have been studied by angular resolved photoemission (ARPES), bosonic quasiparticles can be probed by resonant inelastic scattering (RIXS). The orbital, spin and charge degrees of freedom are quantum variables of electrons and have thus their own dynamics. In the same way as a magnon being a collective spin excitation in a magnetically ordered state; in a long-range orbitally ordered system a collective orbital excitation is predicted and its quantized object is known as orbiton.

Half doped manganites represent the prototype of orbitally ordered systems. In these compounds half of the Mn ions are in the Mn³⁺ state that has a $d^4(t_{2g}^3 e_g^1)$ configuration with one of the two e_g orbitals being occupied by an electron providing an orbital degree of freedom. Hole doping changes the ground state due to the double-exchange interaction and at half doping orbital order (OO) is formed[1]. Due to the strong electron-electron correlation, the theoretical description of the manganite systems is not straightforward. Even though some techniques, like Raman scattering[2] and pump probe experiments[3] have claimed to have observed collective orbital excitations in manganites, these results are controversial[4] as these experiments cannot provide information on the momentum dependence of orbitons.

In the last years, resonant elastic x-ray scattering (REXS) has provided more information about orbital physics by directly observing the orbital order in different manganite compounds[5–14]. However, the dynamics of the orbital degree of freedom is still far from understood. Several theoretical studies have predicted that orbital excitations are distinguishable by characteristic variations in the RIXS amplitude as a function of incident energy and momentum transfer[15–17] from other excitations in the solid. These studies predict that both single- and double-orbiton excitations are allowed, with intensities that are of the same order. In one-dimensional cuprates, orbitons are one of the three quasiparticles that electrons in solids are able to split into during the process of spin-charge separation. In two-dimensional cuprates, pure dispersive orbital excitations have been observed by RIXS [18]. However, the detection and study of the dispersion of orbitons in one of the prototypical orbital ordered materials, i.e. half doped manganites has been elusive so far. To our knowledge only K -edge RIXS studies of doped manganites can be found in the literature to date[19–22]. As RIXS experiments at the K -edge probe the 3d states indirectly[22], studies at the Mn $L_{2,3}$ -edge of doped manganites with high energy resolution are required to bring light into this issue.

The half doped SmBaMn₂O₆ (SBMO) manganite crystallizes in the slightly distorted perovskite structure ABO₃ depicted in Figure 1(a). In this compound the MnO₂ octahedra are sandwiched by two distinct layers built of SmO and BaO[23] in contrast to the disordered Sm_{0.5}Ba_{0.5}MnO₃ (Figure 1(b)) with a random distribution of Sm and Ba ions. The A-site ordered RBaMn₂O₆

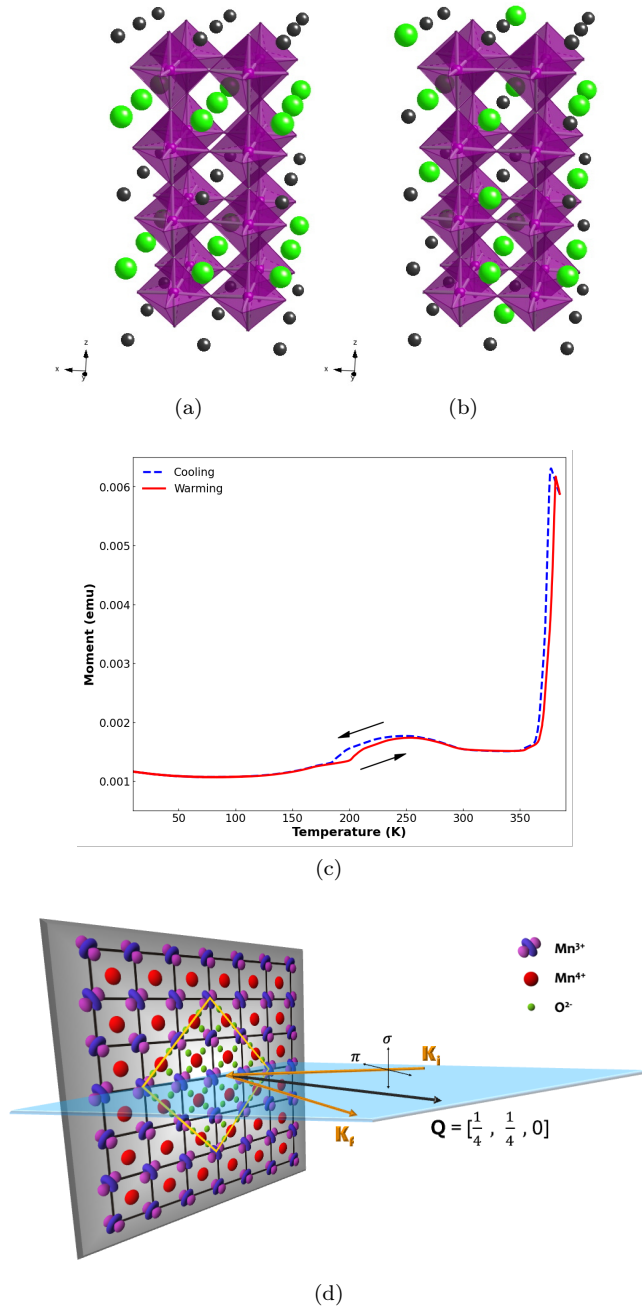


Figure 1: (a) Crystal structure of A-site ordered SBMO. (b) Crystal structure of the disordered $\text{Sm}_{0.5}\text{Ba}_{0.5}\text{MnO}_3$. (c) Magnetization measured as function of temperature. (d) Experimental geometry, the blue plane represents the horizontal scattering plane.

compounds with $R=\text{Sm, Eu, Gd, Tb, Dy, Ho}$ and Y undergo a two-step charge-orbital order (COO) transition at temperatures $T_{co1} = 380$ K and $T_{co2} = 210$ K. Figure 1c shows magnetization measurements of SBMO single crystal where these transitions can be identified. Below $T_{co2} = 210$ K, a disappearance of the simple perovskite

four-fold periodicity along the c -axis has been suggested to be caused by the re-stacking of the COO planes. The exact model, however, remains controversial[24–28]. The issue of the unresolved models arises partly from the fact that most experimental studies were performed on polycrystalline samples which limits the direct observation of its microscopic physical properties. A recent convergent beam electron diffraction experiment on a single crystal of A-site ordered SBMO determined that the space group for the $T_{co2}\text{-COO}$ and $T_{co1}\text{-COO}$ phases are $P21am$ and $Pnam$ respectively [29]. This space group change suggests that an even more complex structural arrangement occurs below T_{co2} as a consequence of the stacking of the COO. Some theoretical studies even predict a ferroelectric state in analogy to $\text{Pr}(\text{Sr}_{0.1}\text{Ca}_{0.9})_2\text{Mn}_2\text{O}_7$ [29, 30]. The existence of this second charge order transition at 210 K, unique for the A-site ordered manganites is responsible for a distinct temperature dependence of the OO parameter that will be discussed later.

In this paper we present REXS and RIXS data which observe the orbital order and its low energy excitations in a single crystal of SBMO. We employ REXS in the vicinity of the Mn $L_{2,3}$ edges to compare the OO signal to the previously published results on powder samples[10, 11]. Using high-energy-resolution RIXS at these edges, we explore the existence of orbitons and other low energy excitations.

Our results show that with the current available energy resolution no orbiton could be detected in this compound at the OO ordering wave vector. However, for deviating momentum transfers, several low energy excitations could be observed that exhibit correlations with the compound’s electronic ordering phenomena.

We observed rich low-energy excitations up to ~ 200 meV at Mn L_3 and L_2 edges. Comparing to the results obtained from Raman scattering and inelastic neutron scattering, the RIXS lower-energy excitations comprise at least magnons and phonons. However, the integrated spectral weight between 80 and 200 meV follows the distinct temperature evolution of the OO peak in A-site ordered manganites, suggesting the possible existence of orbitons in SBMO.

II. EXPERIMENTAL DETAILS

Single-crystalline SBMO was prepared in the following way: the mixed powders were calcined at 1273 K in air, pressed into a rod, and sintered at 1693 K under Ar atmosphere. At first, an A-site alloyed crystal of $\text{Sm}_{1/2}\text{Ba}_{1/2}\text{MnO}_3$ was grown at a rate of 4–10 mm/h in air by a floating-zone method. The melt-quenched crystal was treated in Ar atmosphere at 1693 K for 10 h to encourage the A-site ordering, and then annealed in O_2 at 973 K for 2 h. The structural characterization was performed by x-ray diffraction on a small part of the powdered crystal. The Rietveld analysis with Rietan2000 indicated the perfect ordering of the Sm and Ba

atoms[28]. The magnetic and transport properties of the studied sample were characterized using a SQUID magnetometer and are presented in Figure 1c. The crystal orientation was determined by a lab-based Laue diffractometer prior to the RIXS and REXS experiments.

The RIXS and REXS experiments were conducted at the I21-RIXS beamline at Diamond Light Source, United Kingdom[31]. The sample was mounted with the [110] plane lying in the scattering plane onto a copper sample holder fixed to a liquid He flow cryostat which achieves temperatures between 7 K and 380 K. Experiments were performed using linear horizontal or vertical polarized light leading to π or σ incident photon polarization in respect to the horizontal scattering geometry.

We tuned the incident photon energy to the resonance of the Mn $L_{2,3}$ absorption edges for the RIXS measurements. The total energy resolution achieved was about 24 meV FWHM. RIXS and REXS signals were collected without polarization analysis. For all RIXS spectra, the elastic (zero-energy loss) peak positions were determined by the elastic scattering spectrum from carbon tape placed near the sample surface and then fine adjusted by its Gaussian fitted elastic peak position. The Miller indices in this study are defined with reference to the crystal structure $a_p \times a_p \times 2a_p$ with $a_p \approx 3.9\text{\AA}$ being the cubic perovskite unit cell. The experimental geometry of the sample is depicted in Figure 1(d). The temperature of the measurements was 15 K unless otherwise stated. The REXS measurements were performed using a rotating photodiode inside the sample vessel. The RIXS measurements were collected through continuous rotation of the spectrometer arm due to the 3D nature of the investigated compound. The diffraction peaks have been analyzed using Pseudo-Voigt functions while the inelastic peak were described using Gaussian functions.

III. RESULTS AND DISCUSSION

Figure 2 shows the REXS data of energy dependence of the orbital $(1/4\ 1/4\ 0)$ reflection in the vicinity of the Mn $L_{2,3}$ edges. The insert of Figure 2 shows the comparison to the experimental x-ray absorption (XAS). Clearly, the resonant reflection intensity across the Mn $L_{2,3}$ edges is distinct from the XAS signal and evidences the OO [10, 11, 14]. More specifically, the present measurements on SBMO shows the same differences with the layered $\text{La}_{0.5}\text{Sr}_{1.5}\text{MnO}_4$ spectra observed previously in literature [10]. These differences confirm that the OO of the e_g electrons is of x^2-z^2/y^2-z^2 type in A-site ordered SBMO, while a $3x^2-r^2/3y^2-r^2$ type of orbital order is present in the layered manganite.

Following the REXS measurements, we performed RIXS measurements for various incident energies with the θ and 2θ angles ensuring a fixed momentum transfer at the $(1/4\ 1/4\ 0)$ reflection when varying the x-ray energy. The integrated intensities between 0 and 100 meV of these RIXS spectra are shown as red dots in Figure 2

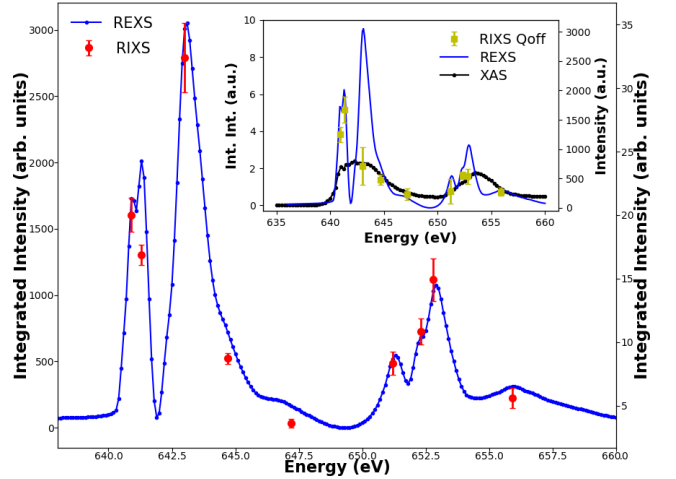


Figure 2: Energy dependence of the $(0.25, 0.25, 0)$ OO reflection together with the integrated intensity of the RIXS signal collected for different incident energies while maintaining the momentum transfer \mathbf{q} constant. The insert shows the XAS taken in fluorescence mode together with the energy dependence of the Q_{off} reflection. The measurements were performed with σ incident polarization at $T = 15\text{K}$.

together with the REXS signal. The measurements are plotted in different y-axis for clarity. Both RIXS and REXS signals are very similar confirming the excellent alignment of the spectrometer arm to $\mathbf{q}_{OO} = (0.25, 0.25, 0)$.

Figure 3 shows interesting information regarding the collected RIXS spectra, the difference of spectral weight between the measurements done at the L_3 and L_2 edges. Due to the self absorption, while the L_2 RIXS spectra shows more clearly the d-d and low energy excitations, the L_3 spectra is mainly dominated by the elastic signal. Keeping this information in mind we proceeded to study the low-energy excitations in order to explore the potential existence of the collective orbiton.

We now discuss the inelastic excitation at the OO $\mathbf{q}_{OO} = (0.25, 0.25, 0)$. Given that the inelastic signal is stronger at the Mn L_2 edge compared to the L_3 edge, we collected the momentum-dependent RIXS spectra across the OO scattering peak at the Mn L_2 edge. Figures 4a and 4b, show the momentum-dependent RIXS maps probed by the linear π and σ incident polarizations, respectively. However, the OO elastic scattering signal completely dominates the spectra with no appreciable spectral weight from the low energy excitations. The low energy excitation spectra between 0 and 200 meV at three different \mathbf{q} positions $(0.25, 0.25, 0)$, $(0.245, 0.245, 0)$ and $(0.255, 0.255, 0)$ and $T=15\text{K}$ are shown in Figure 5. In the normalized plot (upper insert) weak low energy excitations can be observed at around 80 meV when \mathbf{q} is not exactly at the OO Bragg condition. To examine further whether there are any detectable low-energy excitations resonating with the OO peak, we show in the lower inset

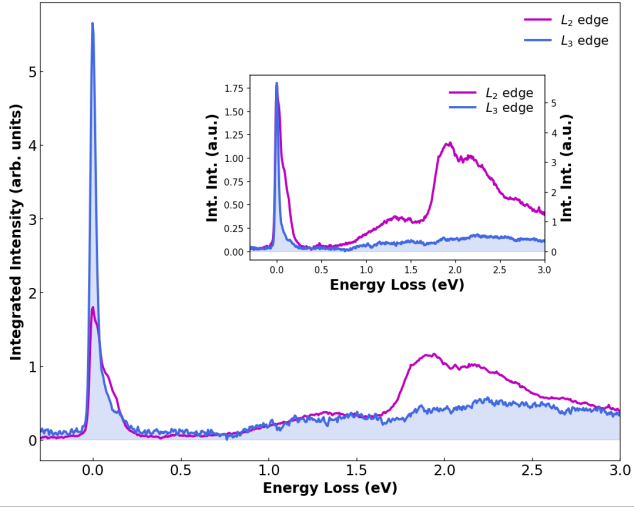


Figure 3: Low energy-transfer RIXS line spectrum measured at the Mn L_2 and L_3 edge with σ incident polarization and $T=15\text{K}$ plotted in different axis. The \vec{q} vector for these measurements corresponds to $(0.2347, 0.2347, -0.0130)$

of Figure 5 the normalized RIXS spectra with incident π and σ polarizations together with the elastic scattering spectrum from a carbon reference sample collected in the same geometry. The nearly identical spectra between the manganite and the reference sample suggest that any possible low-energy excitations are shadowed by the OO scattering at this wave vector.

The RIXS spectra were collected both at the OO condition $\mathbf{q}_{OO} = (0.25, 0.25, 0)$ and off this condition in order to extract the intensity of the low energy excitations. The offsets in tilt and θ angles were increased to achieve an alignment of $\mathbf{q}_{Off} = (0.2347, 0.2347, -0.0130)$. RIXS spectra were collected for the same energy values as the data presented in Figure 2, while varying the experimental geometry to ensure \mathbf{q}_{Off} is preserved for each energy value. The integrated intensity of these RIXS spectra is shown in the insert of figure 2 together with the XAS signal.

The RIXS data at \mathbf{q}_{Off} are shown in figure 6, where several low-energy excitations are visible. We describe the spectra using five gaussian functions while the elastic peak is described with a Pseudo-Voigt function. The available energy resolution does not allow for an univocal fit of the data and different solutions with similar fitting errors can be achieved. However, all the tested fit solutions point into the direction that the observed peaks are not higher harmonics from one another.

These results are interesting when compared to results from inelastic neutron scattering, [32] which studied the magnetic excitations of the canonical half-doped manganite $\text{Pr}_{0.5}\text{Ca}_{0.5}\text{MnO}_3$ in its magnetic and orbitally ordered phase. The neutron study demonstrated the existence of four gapped dispersive magnon modes. By using an effective Heisenberg-Hamiltonian model $\mathcal{H} =$

$-\sum_{\langle ij \rangle} J_{ij} S_i S_j$, the magnon dispersion and the dynamical structure factor were calculated. The gapped spin wave dispersion is consistent with the Goodenough model with strong nearest-neighbor ferromagnetic interactions along the zigzag chains and weak antiferromagnetic interactions between them.

Given the same magnetic structure between PCMO and SBMO, we used the Heisenberg Hamiltonian and the optimized exchange parameters obtained from PCMO to mark the magnetic excitations of SBMO at the given momentum transfer. The obtained energies for the magnon excitations for \mathbf{q}_{Off} are $E_{m_1} = 2 \text{ meV}$, $E_{m_2} = 33.09 \text{ meV}$, $E_{m_3} = 46.62 \text{ meV}$ and $E_{m_4} = 71.98 \text{ meV}$ as displayed in figure 6 by dashed orange lines.

In addition to the magnons, we expect also phonons to be present in this range of energy. Akahoshi et al. [28] studied SBMO using optical conductivity and Raman scattering. These techniques are restricted to collect data at $\mathbf{q} = 0$ and are not sensitive to the dispersion of the observed excitations. Two major peaks are observed in the Raman spectra around 500 and 620 cm^{-1} (62 and 77 meV) that are assigned to the Jahn-Teller (JT) and breathing modes respectively. These phonon energies are displayed in Figure 6 as dashed grey lines.

To better understand the origin of the low energy excitations, we probed its dispersion by collecting its momentum-dependence between $\mathbf{Q} = 0.4864$ and $\mathbf{Q} = 0.8453$ with σ incident polarization at $T=15\text{K}$. The collected RIXS spectra are presented in Figure 7 and are vertically displaced for clarity. The intensity of the RIXS spectra are normalized by the d-d excitations as these are not expected to be dispersive or have significant structure factor modulations. The momentum-dependent low-energy modes do not show sizable dispersion. Four dashed lines represent the calculated dispersion of the magnetic excitations. The comparison demonstrates that the magnons very likely contribute to the low-energy excitations in RIXS. However, other modes, including phonons and orbitons, likely also contribute to the RIXS spectra as the calculated magnon peaks cannot reconcile the observed evolution of low-energy excitations.

Another way to differentiate between these modes is to study their temperature evolution. Figure 8a shows the RIXS spectra at the Mn L_2 edge at \mathbf{q}_{Off} for three different temperatures. Comparing with the temperature dependence of the magnetization recorded during cooling and heating of SBMO presented in figure 1c, allows us to establish the correlation between the RIXS signal and the phase diagram. The three chosen temperatures are $T = 15 \text{ K}$ corresponding to the T_{CO2} phase, $T=300 \text{ K}$ with $T_{CO2} < T < T_{CO}$ and finally at $T=380 \text{ K}$ that is above the metal to insulator transition $T > T_{CO}$.

There are two regions in the spectra that exhibit opposite temperature dependence. Below 50 meV, the intensity of the elastic and lowest energy excitations increases with increasing temperatures. However, for intensities above 50 meV we observe a drastic intensity reduction up

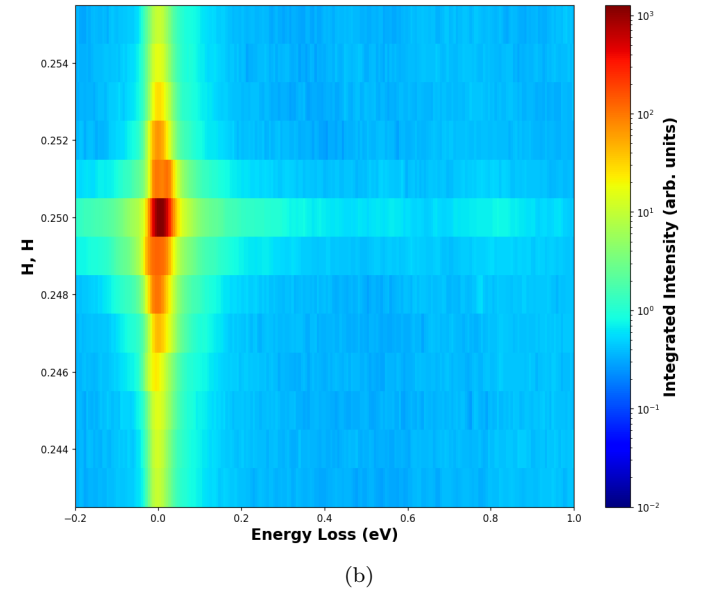
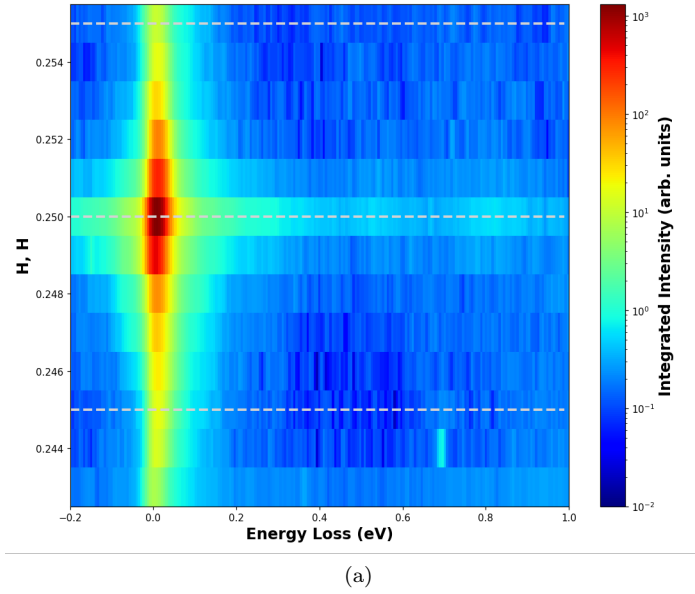


Figure 4: Low energy excitations of SBMO measured in the vicinity of the OO (0.25, 0.25, 0) reflection revealed by Mn L_2 RIXS and $T = 15$ K. (a) Incident π polarization. (b) Incident σ polarization.

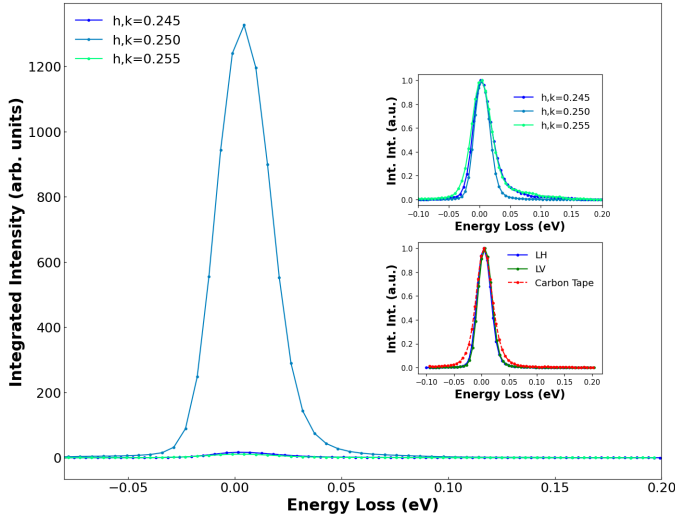


Figure 5: Comparison of RIXS spectra collected at different \mathbf{q} values. The upper insert shows the comparison of the normalized signals while the lower insert shows the comparison of the spectra collected at the OO reflection for both incident polarizations together with the spectrum of a carbon tape measured at the same experimental conditions.

to $T = 300$ K and $T = 380$ K. The temperature evolution of the RIXS spectra is in agreement with Raman which reported that both, the JT and the breathing modes are rapidly suppressed with increasing temperature towards T_{CO2} and bear little intensity in the temperature range of $T_{CO2} < T < T_{CO}$. Remarkably, we observe the pres-

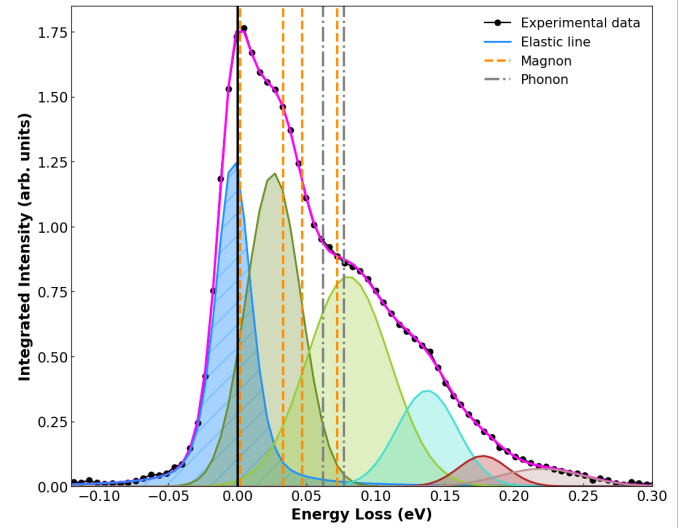


Figure 6: Low energy-transfer RIXS spectrum measured at the Mn L_2 edge with σ incident polarization at $T=15$ K. The \mathbf{q} vector corresponds to (0.2347, 0.2347, -0.0130) and the fits represent an elastic line and five low energy excitations.

ence of several excitations around 100 meV whose energies do not correspond either to magnons or phonons. These excitations exhibit a more pronounced temperature dependence. Ishihara et al [33], postulated in their theoretical study of orbital excitations in LaMnO_3 , that the orbiton energy is of the order of J and larger than the Jahn-Teller phonon energy. Hence, the observed excitations around 100 meV might correspond to orbital

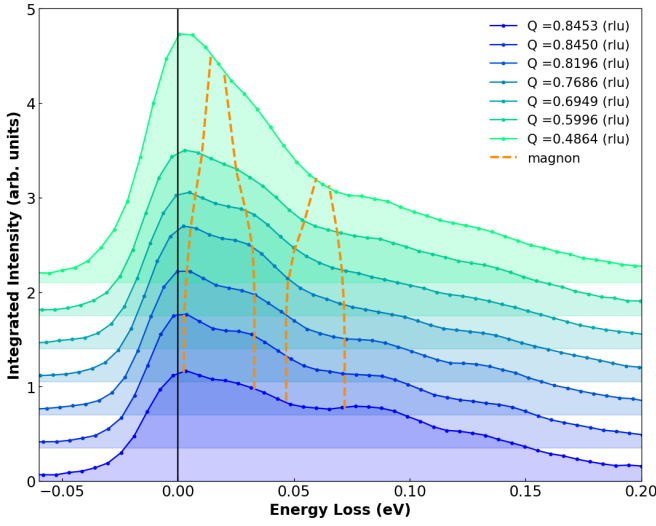


Figure 7: RIXS spectra taken at the Mn L_2 edge with σ incident polarization at $T=15$ K and at different \mathbf{q} vectors. The dashed lines represent the dispersion of the magnon energies for the same \mathbf{q} vectors obtained from theoretical calculations.

excitations. In order to test this scenario, we collected RIXS spectra at further temperatures and we compared its spectral weight around 100 meV with the temperature dependence of the orbital order reflection. The RIXS spectra was fitted using a skewed Gaussian peak to describe the elastic signal and two Gaussian peaks to describe the inelastic low energy excitations. The first Gaussian peak was used to describe the excitations below 50 meV, that as 8a shows increase in intensity with increasing temperature. The second Gaussian peak describes the energy region between 50 meV and 200 meV that exhibits a decreasing spectral weight as function of raising temperature. Figure 8b compares the integrated intensity of the REXS signal as function of temperature with the integrated intensity of the inelastic excitations between 50 meV and 200 meV. A remarkable agreement in their temperature dependence can be observed.

One of the specific properties of the A-site ordered manganites is the transition at $T_{CO2} = 210$ K associated with a change in the stacking of the orbitally ordered planes along the z axis. In the OO temperature dependence it results in a steep increase of intensity by a factor of two. This peculiar behavior was already observed in a previous REXS study of SBMO powder samples [10] and appears also in our REXS measurements of this single crystal. Remarkably, the temperature dependence of the integrated intensity of the excitations around 100 meV follows also this behavior, including the doubling of intensity compared to below T_{CO2} which indicates a correlation between orbital order and the excitations. This evolution is in strong contrast with the one of the excitations at energies below 50 meV.

Several works have considered orbital excitations in

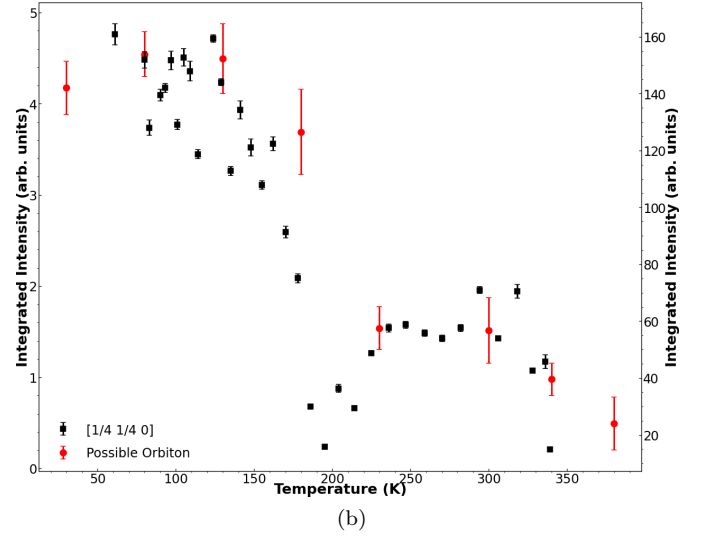
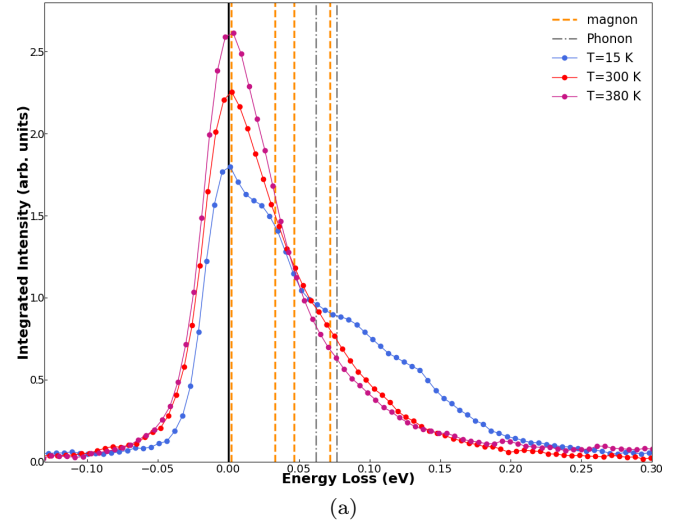


Figure 8: (a) RIXS spectra measured at the Mn L_2 edge and $\mathbf{q}_{Off} = (0.2347, 0.2347, -0.0130)$. The spectra were collected with σ incident polarization and temperatures of 15 K, 300 K and 380 K. (b) Comparison of the integrated intensity of the (0.25, 0.25, 0) orbital order peak measured by REXS with the integrated intensity of the energy excitations between 80 and 200 meV in the RIXS spectra.

the parent compound LaMnO_3 [17, 34–36], with significant variation of the role attributed to phonons. Van der Brink [34] used self-consistent second order perturbation theory in the orbiton-phonon coupling and found that the orbiton dispersion is strongly reduced by the electron-phonon coupling. In addition, he found that this coupling also mixes the orbiton and phonon modes and causes satellite structures in the orbiton and the phonon spectral function. Schmidt et al. [36] performed a calculation to provide information on the nature of orbital excitations in the presence of substantial orbiton phonon coupling. In their model, they considered quantitatively

the dynamic orbiton-phonon interaction that corresponds to the creation or annihilation of a local distortive phonon in the presence of an orbiton. Their results show that the system becomes more local when increasing the orbiton-phonon coupling, i.e., the effective bandwidth of the orbiton band decreases as the orbiton-phonon coupling increases. In a later work, that focussed completely on the observation of orbital excitations in LaMnO_3 using RIXS, Forte et al.[17] used the ultra short core-hole lifetime expansion for RIXS and obtained a gapped orbiton spectrum. Since their calculated orbital Hamiltonian did not have a continuous symmetry, the Goldstone models were absent. In addition they found that at high symmetry points in the Brillouin zone, the intensity of specific orbiton branches vanishes. This result is consistent with our experimental data that shows that at the OO \mathbf{q} vector the OO diffraction peak dominates the spectra. Unfortunately, we are not able to fully separate the contribution of magnons, phonons, and orbitons to the observed spectra. Further experiments using polarization analysis would be required to obtain a clearer picture of the nature of a possible orbiton dispersion in half doped manganite SBMO.

We are aware that these experimental observations are not sufficient to univocally claim that the observed excitations correspond to the elusive orbitons. However, the observed correlation is a strong motivation for further studies. We believe that in order to properly explore the low energy excitations in half doped manganites, further improved energy resolution and additional polarization analysis of the scattered radiation would be essential to clarify the electronic nature of the observed excitations.

IV. CONCLUSIONS

Thanks to the improved flux and energy resolution of new generation soft x-ray RIXS instruments, a re-examination of low energy excitations in half doped A-site ordered SBMO combining RIXS and REXS measurements was performed. At the OO wave vector the OO diffraction peak dominates the spectra completely. When moving slightly away from the Bragg condition, several low energy excitations became observable.

The observed low energy excitations fall within the energy region in which both magnetic and phonon excitations are expected to appear. Comparing to neutron inelastic and Raman scattering results we identified the energies at which magnons and phonons would be expected. We find additional excitations between 80 and 200 meV that could not be identified as magnons or phonons. They could potentially correspond to the elusive orbiton. The temperature dependence of the RIXS and REXS signals shows a clear correlation for the energy excitations between 80 and 200 meV. The unique temperature dependence indicates a clear correlation between orbital order and the excitations. This observed correlation hints to the possibility that these excitations could correspond to the long sought orbiton.

ACKNOWLEDGMENTS

We would like to thank Dr. Russel Ewings for the discussions about the neutron data. We thank Diamond Light Source for the provision of beamtime on beamline I21 under proposals mm24600-1 and mm30866-1 and for access to the facilities of the Materials Characterization Laboratory.

-
- [1] J. van den Brink, G. Khaliullin, and D. Khomskii, *Physical Review Letters* **83**, 5118 (1999).
 - [2] E. Saitoh, S. Okamoto, K. T. Takahashi, K. Tobe, K. Yamamoto, T. Kimura, S. Ishihara, S. Maekawa, and Y. Tokura, *Nature* **410**, 180 (2001).
 - [3] D. Polli, M. Rini, S. Wall, R. W. Schoenlein, Y. Tomioka, Y. Tokura, G. Cerullo, and A. Cavalleri, *Nature Materials* **6**, 643 (2007).
 - [4] M. Grüninger, R. Rückamp, M. Windt, P. Reutler, C. Zobel, T. Lorenz, A. Freimuth, and A. Revcolevschi, *Nature* **418**, 39 (2002).
 - [5] Y. Murakami, H. Kawada, H. Kawata, M. Tanaka, T. Arima, Y. Moritomo, and Y. Tokura, *Physical Review Letters* **80**, 1932 (1998).
 - [6] S. B. Wilkins, P. D. Spencer, P. D. Hatton, S. P. Collins, M. D. Roper, D. Prabhakaran, and A. T. Boothroyd, *Physical Review Letters* **91**, 167205 (2003).
 - [7] K. J. Thomas, J. P. Hill, S. Grenier, Y.-J. Kim, P. Abbamonte, L. Venema, A. Rusydi, Y. Tomioka, Y. Tokura, D. F. McMorrow, G. Sawatzky, and M. van Veenendaal, *Physical Review Letters* **92**, 237204 (2004).
 - [8] S. S. Dhesi, A. Mirone, C. De Nadaï, P. Ohresser, P. Bencok, N. B. Brookes, P. Reutler, A. Revcolevschi, A. Tagliaferri, O. Toulemonde, and G. van der Laan, *Physical Review Letters* **92**, 056403 (2004).
 - [9] U. Staub, V. Scagnoli, A. M. Mulders, K. Katsumata, Z. Honda, H. Grimmer, M. Horisberger, and J. M. Tonnerre, *Physical Review B* **71**, 214421 (2005).
 - [10] M. García-Fernández, U. Staub, Y. Bodenthin, S. M. Lawrence, A. M. Mulders, C. E. Buckley, S. Weyeneth, E. Pomjakushina, and K. Conder, *Phys. Rev. B* **77**, 060402 (2008).
 - [11] M. García-Fernández, U. Staub, Y. Bodenthin, V. Scagnoli, V. Pomjakushin, S. W. Lovesey, A. Mirone, J. Herrero-Martín, C. Piamonteze, and E. Pomjakushina, *Phys. Rev. Lett.* **103**, 097205 (2009).
 - [12] T. A. W. Beale, S. R. Bland, R. D. Johnson, P. D. Hatton, J. C. Cezar, S. S. Dhesi, M. v. Zimmermann, D. Prabhakaran, and A. T. Boothroyd, *Physical Review B* **79**, 054433 (2009).
 - [13] U. Staub, M. García-Fernández, Y. Bodenthin, V. Scagnoli, R. A. De Souza, M. Garganourakis,

- E. Pomjakushina, and K. Conder, *Physical Review B* **79**, 224419 (2009).
- [14] M. García-Fernández, U. Staub, Y. Bodenthin, V. Pomjakushin, A. Mirone, J. Fernández-Rodríguez, V. Scagnoli, A. M. Mulders, S. M. Lawrence, and E. Pomjakushina, *Phys. Rev. B* **82**, 235108 (2010).
 - [15] S. Ishihara and S. Maekawa, *Phys. Rev. B* **62**, 2338 (2000).
 - [16] S. Ishihara, H. Kondoh, and S. Maekawa, *Physica B: Condensed Matter* **345**, 15 (2004), proceedings of the Conference on Polarised Neutron and Synchrotron X-rays for Magnetism.
 - [17] F. Forte, L. J. P. Ament, and J. van den Brink, *Phys. Rev. Lett.* **101**, 106406 (2008).
 - [18] J. Schlappa, K. Wohlfeld, K. J. Zhou, M. Mourigal, M. W. Haverkort, V. N. Strocov, L. Hozoi, C. Monney, S. Nishimoto, S. Singh, A. Revcolevschi, J. S. Caux, L. Patthey, H. M. Rønnow, J. van den Brink, and T. Schmitt, *Nature* **485**, 82 (2012).
 - [19] H. Kondo, S. Ishihara, and S. Maekawa, *Phys. Rev. B* **64**, 014414 (2001).
 - [20] T. Inami, T. Fukuda, J. Mizuki, S. Ishihara, H. Kondo, H. Nakao, T. Matsumura, K. Hirota, Y. Murakami, S. Maekawa, and Y. Endoh, *Phys. Rev. B* **67**, 045108 (2003).
 - [21] K. Ishii, T. Inami, K. Ohwada, K. Kuzushita, J. Mizuki, Y. Murakami, S. Ishihara, Y. Endoh, S. Maekawa, K. Hirota, and Y. Moritomo, *Phys. Rev. B* **70**, 224437 (2004).
 - [22] S. Grenier, J. P. Hill, V. Kiryukhin, W. Ku, Y.-J. Kim, K. J. Thomas, S.-W. Cheong, Y. Tokura, Y. Tomioka, D. Casa, and T. Gog, *Phys. Rev. Lett.* **94**, 047203 (2005).
 - [23] T. Nakajima, H. Yoshizawa, and Y. Ueda, *Journal of the Physical Society of Japan* **73**, 2283 (2004), <https://doi.org/10.1143/JPSJ.73.2283>.
 - [24] M. Uchida, D. Akahoshi, R. Kumai, Y. Tomioka, T.-h. Arima, Y. Tokura, and Y. Matsui, *Journal of the Physical Society of Japan* **71**, 2605 (2002), <https://doi.org/10.1143/JPSJ.71.2605>.
 - [25] H. Kageyama, T. Nakajima, M. Ichihara, Y. Ueda, H. Yoshizawa, and K. Ohoyama, *Journal of the Physical Society of Japan* **72**, 241 (2003), <https://doi.org/10.1143/JPSJ.72.241>.
 - [26] T. Nakajima, H. Kageyama, M. Ichihara, K. Ohoyama, H. Yoshizawa, and Y. Ueda, *Journal of Solid State Chemistry* **177**, 987 (2004).
 - [27] T. Arima, D. Akahoshi, K. Oikawa, T. Kamiyama, M. Uchida, Y. Matsui, and Y. Tokura, *Phys. Rev. B* **66**, 140408 (2002).
 - [28] D. Akahoshi, Y. Okimoto, M. Kubota, R. Kumai, T. Arima, Y. Tomioka, and Y. Tokura, *Phys. Rev. B* **70**, 064418 (2004).
 - [29] D. Morikawa, K. Tsuda, Y. Maeda, S. Yamada, and T.-h. Arima, *Journal of the Physical Society of Japan* **81**, 093602 (2012), <https://doi.org/10.1143/JPSJ.81.093602>.
 - [30] Y. Tokunaga, T. Lottermoser, Y. Lee, R. Kumai, M. Uchida, T. Arima, and Y. Tokura, *Nature Materials* **5**, 937 (2006).
 - [31] K.-J. Zhou, A. Walters, M. Garcia-Fernandez, T. Rice, M. Hand, A. Nag, J. Li, S. Agrestini, P. Garland, H. Wang, S. Alcock, I. Nistea, B. Nutter, N. Rubies, G. Knap, M. Gaughran, F. Yuan, P. Chang, J. Emmins, and G. Howell, *Journal of Synchrotron Radiation* **29**, 563 (2022).
 - [32] R. A. Ewings, T. G. Perring, O. Sikora, D. L. Abernathy, Y. Tomioka, and Y. Tokura, *Phys. Rev. B* **94**, 014405 (2016).
 - [33] S. Ishihara, Y. Murakami, T. Inami, K. Ishii, J. Mizuki, K. Hirota, S. Maekawa, and Y. Endoh, *New Journal of Physics* **7**, 119 (2005).
 - [34] J. van den Brink, *Physical Review Letters* **87**, 217202 (2001).
 - [35] P. B. Allen and V. Perebeinos, *Physical Review Letters* **83**, 4828 (1999).
 - [36] K. P. Schmidt, M. Grüninger, and G. S. Uhrig, *Physical Review B* **76**, 075108 (2007).